

# Hole mobility of cylindrical GaSb nanowires

Francisco G. Ruiz<sup>\*1</sup>, Enrique G. Marín<sup>†2</sup>, Celso Martínez-Blanco<sup>1</sup>, I. M. Tienda-Luna<sup>1</sup>, J. M. Gonzalez-Medina<sup>1</sup>, A. Toral<sup>1</sup>, L. Donetti<sup>1</sup>, A. Godoy<sup>1</sup>

<sup>(1)</sup> Dpto. Electrónica y Tec. Computadores, Fac. de Ciencias, Univ. Granada, Fuentenueva S/N, 18071 Granada, Spain, <sup>(2)</sup> Dpto. di Ingegneria dell'Informazione, Università di Pisa, Via G. Caruso 16, 56122 Pisa, Italy. \*franruiz@ugr.es, †egmarin@ugr.es

**Abstract**—The hole mobility of GaSb field-effect transistor nanowires is analyzed as a function of the device orientation and gate bias. To this purpose, a self-consistent Poisson-Schrödinger solver with an  $8 \times 8$   $k \cdot p$  Hamiltonian is employed to study the electrostatics, and the hole mobility is calculated under the momentum relaxation time solution of the Boltzmann transport equation including the main high-field scattering mechanisms.

**Keywords**- III-antimonides, GaSb, Hole mobility,  $k \cdot p$  simulation, charge screening, phonons, surface roughness, III-V materials

## I. INTRODUCTION

III-V materials constitute an interesting alternative to substitute or augment silicon CMOS technology in future high-speed and low-power logic applications. Indeed, nFETs with InGaAs channels outperforming silicon has already been successfully demonstrated and more recently, fully operative III-V CMOS devices have been experimentally proven. In spite of that, the investigation of the best III-V p-type complement to n-type InGaAs is still open. III-antimonides are revealing as promising contenders. Particularly, GaSb has exhibited high bulk hole mobility, and the fabrication of both, planar devices and nanowires has been recently achieved [1]. Previous works have focused on ultra-thin semiconductor-on-insulator GaSb devices, and analyzed theoretically their mobility as a function of orientation, size and/or strain conditions [2]. Nevertheless, despite their interest in the devices community, there is not a systematic work studying the hole mobility of GaSb nanowires (NWs), which is the main objective of this paper.

## II. NUMERICAL METHOD

First, we calculate the electrostatics of long-channel GaSb nanowires solving an  $8 \times 8$   $k \cdot p$  Hamiltonian self-consistently with the Poisson equation, as described in [3]. Arbitrary orientation is included in the simulations through the rotation of the corresponding Hamiltonian matrix. To evaluate the mobility, we solve the Boltzmann Transport Equation under the Momentum Relaxation Time approximation and make use of the Kubo-Greenwood approach, taking the most relevant scattering mechanisms into account: non-polar acoustic and optical phonons (ACPH, OPPH), polar optical phonons (POP) and surface roughness (SR) scattering. For ACPH and OPPH, the calculation of the scattering matrix is performed as described in Martínez-Blanco et al. [4], including the dependence of the wavefunction with the wavevector  $k$ . On the contrary, for POP and SR scattering mechanisms, the calculations are simplified

considering the wavefunctions at  $k=0$ , in order to save computational burden. The evaluation of the SR scattering elements is performed as in [5], with  $\Delta_{sr}=0.25\text{nm}$  and  $L_{sr}=1.5\text{nm}$ , whereas the numerical determination of the spatial integrals is performed employing the Fast-Fourier Transform as proposed by Stanojevic et al. [6]. Moreover, dielectric screening is included in the calculation of the SR scattering. So, we follow the approach by Jin et al. [7], considering only intra-subband interactions in the screening matrix. In this calculation, the wavefunctions at  $k=0$  are taken into account.

## III. RESULTS

We study the hole mobility in GaSb cylindrical nanowires oriented along [001], [011] and [111] crystallographic axis. As long-channel devices are considered, only the semiconductor radius ( $R_s=5\text{nm}$ ) and the insulator thickness ( $T_{ins}$ ) are needed to fully define the structure.  $\text{Al}_2\text{O}_3$  is used as gate insulator, with  $T_{ins}=1.5\text{nm}$ . Figure 1 shows the mobility as a function of the carrier density  $P_i$ . The three channel orientations considered are included, and the total, SR-limited, and ACPH-limited mobilities specified. The behavior of POP and OPPH-limited mobilities follow that of ACPH but are less limiting and have therefore not been depicted. As can be observed, there is a considerable impact of the channel orientation on the mobility and, more importantly, quite different trends on the surface-roughness and the phonon-limited mobilities.

- i) The [001]-oriented device attains the lowest phonon mobility. This behavior is related to the fact that [011] and [111]-oriented devices show a sharper band profile close to the valence band limit (see Fig. 2, where the band structure at  $V_G=-1\text{V}$  is represented).
- ii) On the other hand, SR-limited mobility is much larger for the [001]-oriented nanowire than for [011] and [111] devices, in particular for high  $P_i$  values. To explain this trend, we have studied the charge distribution, which is critical to determine SR behavior. Figure 3 depicts the charge density for the three devices under consideration at  $V_G=-1\text{V}$ , which turns out to be strongly anisotropic. Thus, it is not easy to analyze the position of the charge, so we have depicted three slices of the charge distribution taken at different angles (Fig. 4), which reveal that the charge distribution is furthest from the semiconductor/insulator interface in the [001]-oriented device, diminishing the SR influence and therefore explaining the presented results.

iii) The effects of SR and phonons tend to balance at low carrier densities, and the three orientations result in mobilities close to  $2 \times 10^3 \text{ cm}^2/\text{eV}\cdot\text{s}$ . For higher bias (and carrier densities), SR becomes the dominant mechanism because of the charge redistribution in the nanowire, and large differences are observed amongst crystal orientations, with the [001] device mobility at least doubling those of [011] and [111] devices.

#### ACKNOWLEDGMENT

The authors acknowledge the support by the Spanish Government under the Project TEC2014-59730-R. A. Toral and J M González-Medina acknowledge grants FPU16/04043 and FPU014/02579, respectively.

#### REFERENCES

- [1] Z. Yang et al., “Complementary Metal Oxide Semiconductor-Compatible, high-mobility, 111-oriented GaSb nanowires enabled by Vapor-Solid-Solid Chemical Vapor Deposition”, ACS Nano, 11 (4), 2017.
- [2] P. Chang, X. Liu, G. Du and X. Zhang, “Assessment of hole mobility in strained InSb, GaSb and InGaSb based ultra-thin body pMOSFETs with different surface orientations”, Proc. IEDM 2014.

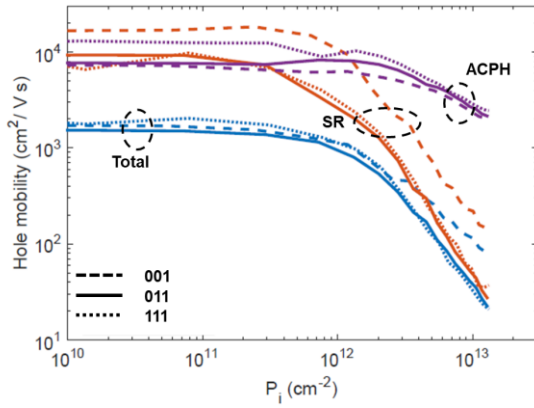


Figure 1. Total, ACPH and SR-limited mobility vs.  $P_i$  for [001], [011] and [111]-oriented GaSb NWs.

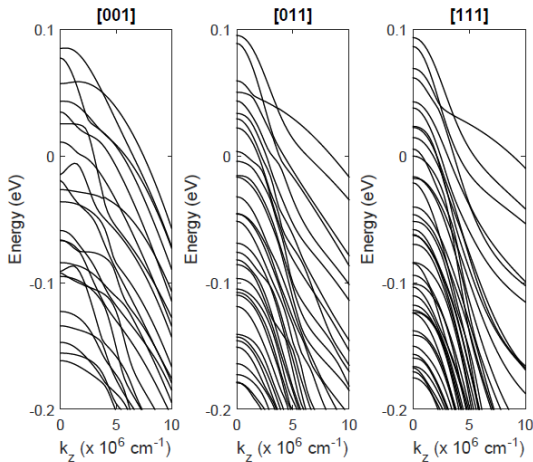


Figure 2. Band structure of  $R_s=5\text{nm}$  GaSb NWs with three different transport orientations at  $V_G = -1\text{V}$ .

- [3] C. Martinez Blanque et al., “Electrostatic performance of InSb, GaSb, Si and Ge p-channel nanowires”, J. Phys. D: Appl. Phys. 50, 495106, 2017.
- [4] C. Martinez-Blanque et al., “Influence of alloy disorder scattering on the hole mobility of SiGe nanowires”, J. App. Phys., 116, 244502 (2014).
- [5] S. Jin et al., “Coupled Drift-Diffusion (DD) and Multi-Subband Boltzmann Transport Equation (MSBTE) solver for 3D Multi-Gate Transistors”, Proc. SISPAD 2013.
- [6] Z. Stanojevic and H. Kosina, “Surface-Roughness-Scattering in non-planar channels – the role of band anisotropy”, Proc. SISPAD 2013.
- [7] S. Jin, M. V. Fischetti and T. Tang, “Modeling of electron mobility in gated silicon nanowires at room temperature: Surface roughness scattering, dielectric screening, and band nonparabolicity”, J. App. Phys., 102, 083715 (2007).

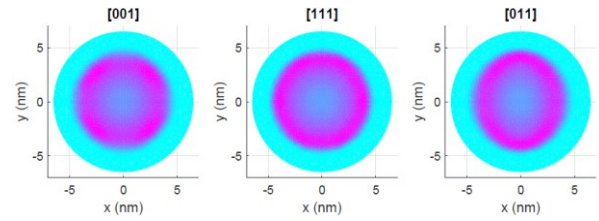


Figure 3. Hole density for the three orientations under consideration at  $V_G=-1\text{V}$ .

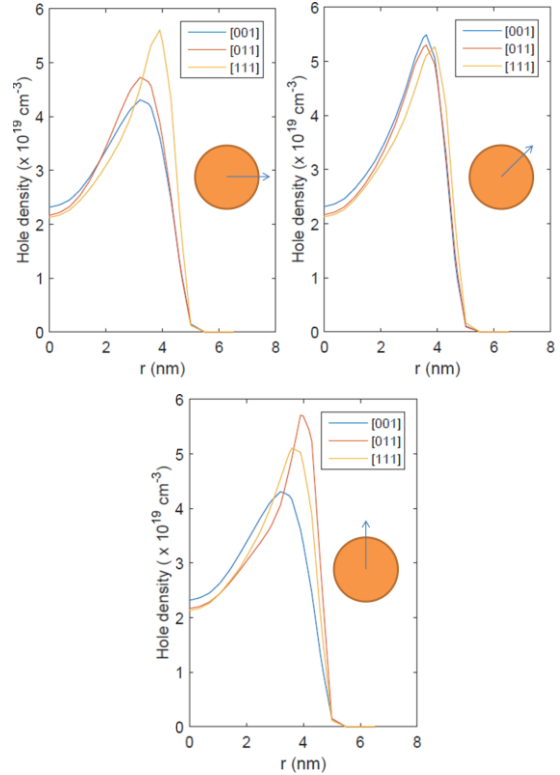


Figure 4. Hole density for different-oriented GaSb NWs at  $V_G = -1\text{V}$  (the directions for each slice are depicted in the insets, to account for anisotropic charge).